

Electronic Supporting Information

Pressure-induced chemistry for the 2D to 3D transformation of zeolites

Michal Mazur,* Angel M. Arévalo-López, Paul S. Wheatley, Giulia P. M. Bignami, Sharon E. Ashbrook, Ángel Morales-García, Petr Nachtigall, J. Paul Attfield, Jiří Čejka, and Russell E. Morris

Abstract: ADOR, an unconventional synthesis strategy based on a four-step mechanism: assembly, disassembly, organization, and reassembly, has opened new possibilities in zeolite chemistry. The ADOR approach led to discovery of IPC family of materials with tuneable porosity. Here we present the first pressure-induced ADOR transformation of the 2D zeolite precursor IPC-1P into fully crystalline 3D zeolite IPC-2 (**OKO** topology) using a Walker-type multianvil apparatus under pressure of 1 GPa at 200 °C. Surprisingly, the high-pressure material is of lower density (higher porosity) than the product from simply calcining the IPC-1P precursor at high temperature, which produces IPC-4 (**PCR** topology). The sample was characterized by PXRD, ²⁹Si MAS NMR, SEM, and HRTEM. Theoretical calculations suggest that high pressure can lead to the preparation of other ADOR zeolites that have not yet been pre-pared.

*e-mail: mm402@st-andrews.ac.uk

Experimental Procedures

MATERIALS

SYNTHESIS OF ZEOLITE UTL AND THE LAYERED PRECURSOR IPC-1P

For the synthesis of **UTL** parent zeolite the procedure from Ref. [1] was used. Reaction mixture with the following molar ratio was used to prepare parent **UTL** zeolite: 1.0SiO₂: 0.5GeO₂: 0.2ROH/Br: 37.5H₂O, where ROH is the SDA: (6R,10S)-6,10-dimethyl-5-azoniaspiro[4,5]decane hydroxide. In the standard procedure, the SDA in bromide form (46.70 g) was dissolved in the distilled water (250 g) and stirred with resin (Bio-Rad AG 1-X8, 80 g) for 4 h to exchange it to hydroxide form. After separation of resin, the crystalline germanium oxide (19.38 g) and silicon dioxide (Cab-O-Sil® M5, 22.25 g) was introduced, and the mixture was homogenized for 30 min at room temperature. The resulting fluid gel was charged into Teflon-lined autoclave and heated at 175 °C for 7 days under agitation (25 rpm). The solid product was recovered by filtration, washed with distilled water, and dried at 60 °C.

To remove the SDA, the as-synthesized zeolite was calcined in a stream of air at 550 °C for 8 h with a temperature ramp of 1 °C/min.

Calcined **UTL** was hydrolyzed in 0.1 M HCl with w/w ratio of 1/200 at 95 °C under reflux, for 16 h. The solid product (IPC-1P) was isolated by filtration and centrifugation, washed with water, centrifuged again, and dried in air [2].

PRESSURE-INDUCED ADOR TRANSFORMATION

The IPC-1P to IPC-2 transformation was performed in a Walker type multianvil apparatus [Figure 1.] under high-pressure, high-temperature conditions. 30 mg of the layered precursor were placed inside a Pt capsule. Temperature, pressure and time of the treatments varied for each experiment as shown in the main text. The sample was compressed to the working pressure, then heated following by cooling to room temperature before the pressure was slowly released.

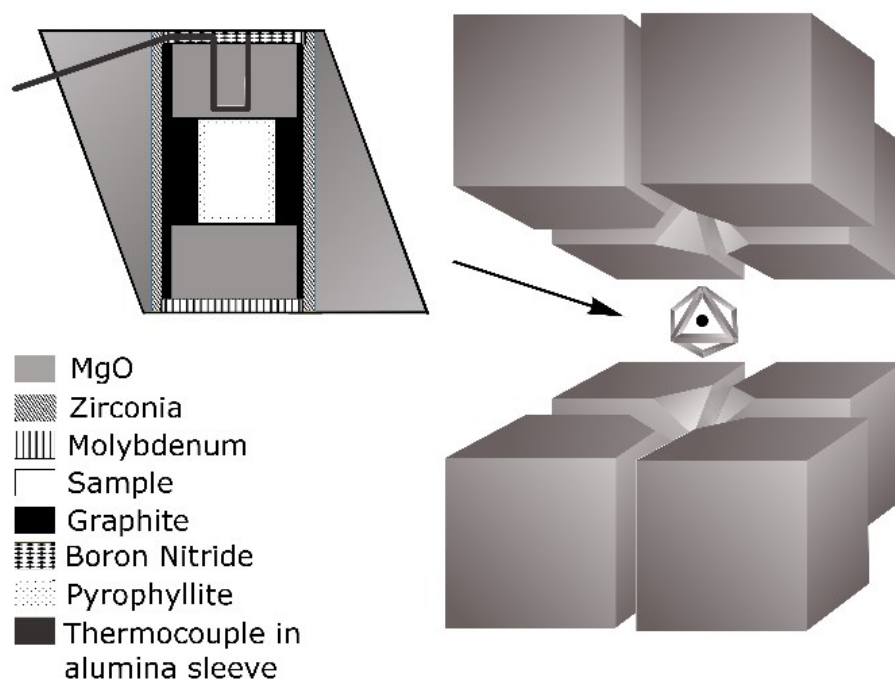


Figure S1. Cross section of the octahedral pressure cell (left) and schematic view of the eight truncated tungsten carbide cubes compressing the octahedron (right) in the Walker-type multianvil apparatus [3].

CHARACTERIZATION METHODS

XRD

X-ray powder diffraction data were obtained on a Bruker AXS D8 ADVANCE diffractometer with a Vantec-1 detector in the Bragg-Brentano geometry using $\text{CuK}\alpha$ radiation. Samples were gently ground using agate mortar to limit the effect of preferential orientation of individual crystals in the sample holder.

ELECTRON MICROSCOPY

The morphology of the crystals was examined by scanning electron microscopy (SEM) using a JEOL JSM-5500LV. The high-resolution transmission electron microscopy (HRTEM) was performed using Jeol JEM-2011 electron microscope operating at an accelerating voltage of 200 kV. The HRTEM images were recorded using a 9 Gatan 794 CCD camera. The camera length, sample position and magnification were calibrated using standard gold film methods.

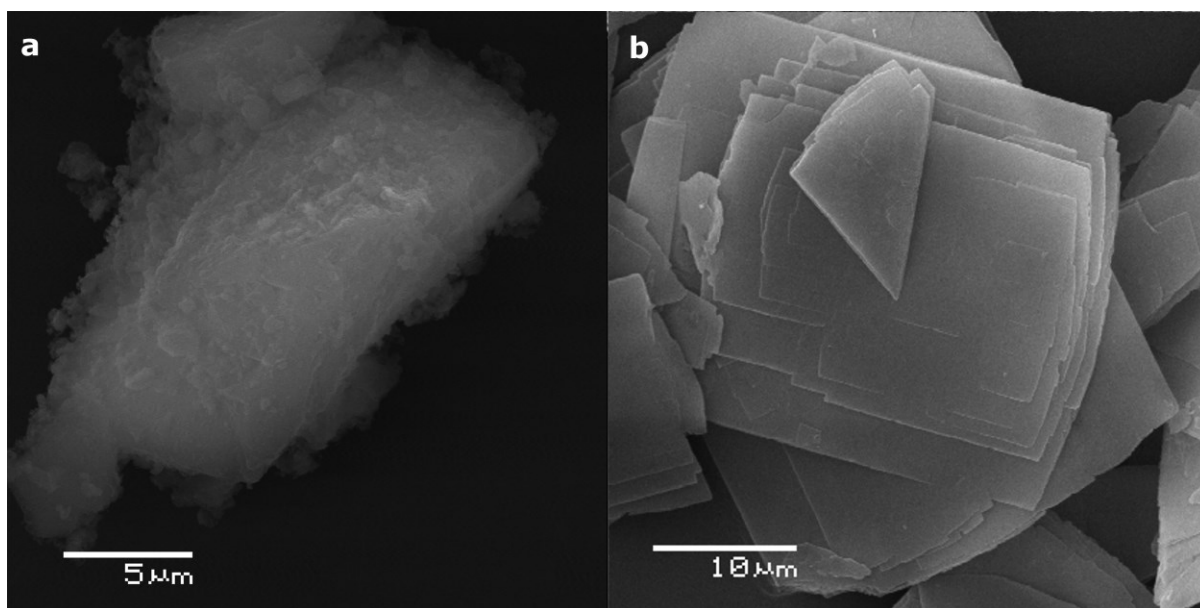


Figure S2. SEM images of IPC-2 zeolite synthesized under high (a) and low (b) pressure. The crystals of the sample obtained by the pressure-induced method have different shape; they are less well defined.

NMR

^{29}Si solid-state NMR spectra were acquired using a Bruker Avance III spectrometer, equipped with a 14.1 T wide-bore superconducting magnet, at a Larmor frequency of 119.3 MHz. The freshly calcined sample available (10 mg) was packed into a 1.9 mm ZrO_2 rotor that was rotated at a rate of 30 kHz, using a 1.9 mm HX probe. Magic angle spinning (MAS) spectra were acquired using a radiofrequency (rf) field strength of ~ 100 kHz, with a repeat interval of 120 s. The Q^4/Q^3 ratio was determined using DMFit [4]. For cross-polarization (CP) [5] experiments, transverse magnetization was transferred (from ^1H) using a contact pulse of 5 ms (ramped for ^1H).

COMPUTATIONAL DETAILS

Periodic Density Functional Theory (DFT) calculations were carried out using the Perdew-Burke-Ernzerhof (PBE) exchange-correlation functional [6] as implemented in the Vienna *ab initio* Simulation Package (VASP) [7]. The plane-wave basis set with the cutoff energy of 600 eV was used and the Brillouin zone was sampled just at the Γ -point. Self-consistency was reached when the total energy changed less than 10^{-6} eV between subsequent cycles; the geometry optimization was stopped when the force on each ion was less than $0.01 \text{ eV } \text{\AA}^{-1}$. The relative enthalpy with respect to the most stable **UTL-S4R** zeolite topology at the atmospheric pressure (**OKO**) are reported as a function of pressure. Full structural relaxations at each pressure were performed via a conjugate gradient minimization of the enthalpy using the Hellmann-Feynman forces on the atoms and stresses on the unit cell.

Table S1. Energy (eV) and volume (\AA^3) for UTL-S4R (P-1, Pm, P1 and Pm') zeolites at the pressure range (0-2 GPa) selected to investigate the energetic stability in terms of Enthalpy vs. pressure in Figure 6.

P / GPa	$V / \text{\AA}^3$	E / eV	$V / \text{\AA}^3$	E / eV	$V / \text{\AA}^3$	E / eV	$V / \text{\AA}^3$	E / eV
	UTL-S4R (P-1)		UTL-S4R (Pm)		UTL-S4R (P1)		UTL-S4R (Pm')	
0	1996.39	-805.5747	1882.17	-802.8344	1832.71	-802.6176	1745.62	-800.1602
1	1924.96	-805.3556	1822.44	-802.6474	1787.14	-802.4786	1690.86	-799.9892
2	1849.17	-804.654	1754.51	-802.0093	1740.61	-802.0431	1627.99	-799.4049

References

- [1] O. V. Shvets, N. Kasian, A. Zukal, J. Pinkas, J. Čejka, *Chemistry of Materials* **2010**, 22, 3482-3495.
- [2] W. J. Roth, O. V. Shvets, M. Shamzhy, P. Chlubná, M. Kubů, P. Nachtigall, J. Čejka, *J. Am. Chem. Soc.* **2011**, 133, 6130-6133.
- [3] H. Huppertz, *Chemical Communications* **2011**, 47, 131-140.
- [4] D. Massiot, F. Fayon, M. Capron, I. King, S. Le Calvé, B. Alonso, J.-O. Durand, B. Bujoli, Z. Gan, G. Hoatson, *Magnetic Resonance in Chemistry* **2002**, 40, 70-76.
- [5] (a) A. Pines, M. G. Gibby, J. S. Waugh, *The Journal of Chemical Physics* **1972**, 56, 1776-1777; (b) S. E. Ashbrook, S. Sneddon, *Journal of the American Chemical Society* **2014**, 136, 15440-15456.
- [6] J. P. Perdew, K. Burke, M. Ernzerhof, *Physical Review Letters* **1996**, 77, 3865-3868.
- [7] (a) G. Kresse, J. Furthmüller, *Computational Materials Science* **1996**, 6, 15-50; (b) G. Kresse, J. Furthmüller, *Physical Review B* **1996**, 54, 11169-11186.